Generation and characterization of antagonistic anti-human interleukin (IL)-18 monoclonal antibodies with high affinity: Two types of monoclonal antibodies against full-length IL-18 and the neoepitope of inflammatory caspase-cleaved active IL-18

Yuko Nariai[a,1], Hiroki Kamino[a,1], Eiji Obayashi[a], Hiroaki Kato[a], Gyosuke Sakashita[a], Tomoko Sugiura[a], Kiyoshi Migita[b], Tomohiro Koga[c], Atsushi Kawakami[c], Kazuma Sakamoto[d], Kenji Kadomatsu[d], Makoto Nakakido[e], Kouhei Tsumoto[e,f], Takeshi Urano[a,g,*]

[a] Department of Biochemistry, Shimane University School of Medicine, Izumo, 693-8501, Japan
[b] Department of Rheumatology, Fukushima Medical University School of Medicine, Fukushima, 960-1247, Japan
[c] Department of Rheumatology, Unit of Advanced Preventive Medical Sciences, Graduate School of Biomedical Sciences, Nagasaki University, Nagasaki, 852-8501, Japan
[d] Department of Biochemistry, Nagoya University Graduate School of Medicine, 65 Tsurumai-Cho, Showa-Ku, Nagoya, 466-8550, Japan
[e] Department of Bioengineering, School of Engineering, The University of Tokyo, Hongo, Bunkyo-ku, Tokyo, 113-8656, Japan
[f] Institute of Medical Science, The University of Tokyo, Shirokanedai, Minato-ku, Tokyo, 108-8639, Japan
[g] mAbProtein Co. Ltd, Izumo, 693-8501, Japan

ABSTRACT

Interleukin-18 (IL-18) is a pro-inflammatory cytokine that evokes both innate and acquired immune responses. IL-18 is initially synthesized as an inactive precursor and the cleavage for processing into a mature, active molecule is mediated by pro-inflammatory caspases following the activation of inflammasomes. Two types of monoclonal antibodies were raised: anti-IL-18[63−68] antibodies which recognize full-length[1−193] and cleaved IL-18; and anti-IL-18 neoepitope antibodies which specifically recognize the new N-terminal [37]YFGKLESK[44] of IL-18 cleaved by pro-inflammatory caspase-1/4. These mAbs were suitable for Western blotting, capillary Western immunoassay (WES), immunofluorescence, immunoprecipitation, and function-blocking assays. WES analysis of these mAbs allowed visualization of the IL-18 bands and provided a molecular weight corresponding to the pro-inflammatory caspase-1/4 cleaved, active form IL-18[37−193], and not to the inactive precursor IL-18, in the serum of patients with adult-onset Still's disease (6/14, 42%) and hemophagocytic activation syndrome (2/6, 33%). These monoclonal antibodies will be very useful in IL-18 and inflammasome biology and for diagnostic and therapeutic strategies for inflammatory diseases.

1. Introduction

Interleukin-18 (IL-18) is a pro-inflammatory cytokine assigned to the IL-1 family because of its structural homology, receptor utilization and signal transduction pathways [1–3]. IL-18 has been shown to be a multifunctional cytokine that awakens both innate and acquired immune responses. Like IL-1β, IL-18 is initially synthesized as an inactive precursor (24 kDa) and the cleavage required for processing into mature 18 kDa IL-18 is mainly mediated by pro-inflammatory caspases following the activation and assembly of macromolecular complexes called inflammasomes [4–6]. Only the mature protein is reported to be biologically active. The activated pro-inflammatory caspases simultaneously cleave gasdermin-D, a pyroptotic membrane pore-forming protein, releasing the N-terminal effector domain from the C-terminal inhibitory domain [7,8]. The N-terminal domain oligomerizes in the cell membrane and forms a pore 10–16 nm in diameter through which smaller diameter substrates such as IL-1β and IL-18 are secreted. The increasing abundance of membrane pores ultimately leads to membrane rupture and inflammatory cell death (pyroptosis), releasing the entire cellular contents [9].

IL-18 is constitutively expressed in monocytes, macrophages, intestinal epithelial cells, dermal keratinocytes, osteoblasts, synovial fibroblasts, and adrenal cortex cells [1]. IL-18 binds specifically to the IL-18 receptor α (IL-18Rα; also known as IL-1Rrp, IL-1R5 or CD218a), which then leads to the recruitment of IL-18Rβ (also known as IL-18RArp, IL-1RAcPL, IL-1R7 or CD218b) and the activation of downstream NF-κB and MAPK pathways [10,11].

IL-18 was found to be associated with or contribute to numerous

inflammatory-associated disorders [3,12–14]. Recently, several new gain-of-function mutations in inflammasome forming protein NLR-family CARD-containing protein 4 (NLRC4) have been identified in humans that cause autoinflammation, with a spectrum of clinical manifestations ranging from urticaria to life-threatening macrophage activation syndrome with severe enterocolitis [15–19]. These NLRC4-associated autoinflammatory disorders (or NLRC4 inflammasomopathies) are characterized by markedly increased IL-18 levels in the serum of patients [20].

Once cleaved through inflammasome activation, the N-terminus of active IL-18 represents a novel epitope not present in normal cells. Therefore, detection of this neoepitope should provide a unique and sensitive indicator of inflammatory action. In the present study, we raised two types of monoclonal antibodies: anti-IL-18$^{63-68}$ antibodies which recognize both full-length and cleaved IL-18; and anti-IL-18 neoepitope antibodies which specifically recognize the new N-terminus of IL-18 following cleavage by pro-inflammatory caspase-1/4.

2. Experimental procedures

2.1. Antibodies

The following commercial antibodies were used: mouse monoclonal anti-G196 (R-G-001, mAbProtein, Shimane, Japan) and rabbit polyclonal anti-G196 (B-G-001, mAbProtein); mouse monoclonal anti-FLAG (M2, Sigma-Aldrich, St. Louis, MO, USA); rabbit polyclonal anti-YKDDDDK-tag (60-031, BioAcademia, Osaka, Japan); horseradish peroxidase (HRP)-conjugated goat F(ab')$_2$ anti-mouse (710–1332, Rockland Immunochemicals, Limerick, ME, USA); HRP-conjugated goat anti-rabbit IgG (H + L) (111-035-003, Jackson ImmunoResearch Laboratories, West Grove, WV, USA); and Alexa 488-conjugated goat anti-mouse IgG (H + L) (A-11029, ThermoFisher Scientific, Waltham, MA, USA).

2.2. Cell culture and transfection

Human embryonic kidney cells (HEK-293) (JCRB9068), HeLa human cervical epithelioid carcinoma (JCRB9004), and KG-1 human acute myeloblastic leukemia (JCRB0065) cells were purchased from the Japanese Collection of Research Bioresources (JCRB) Cell Bank. Human HEK-293 and HeLa cells were grown in DMEM (Nissui, Tokyo, Japan) and hybridomas and KG-1 cells were grown in RPMI1640 medium (ThermoFisher Scientific) supplemented with 10% fetal bovine serum (FBS) (Sigma-Aldrich). HEK-293 and HeLa cells were transiently transfected with each plasmid described below using Lipofectamine 2000 (ThermoFisher Scientific) according to the manufacturer's instructions.

2.3. Plasmid construction and expression

Synthetic genes coding for IL-18$^{2-193}$ (UniProt ID Q14116-1), IL-18$^{37-193}$, IL-1α$^{110-271}$ (P01583-1), IL-1β$^{117-269}$ (P01584-1), IL-1Ra$^{26-177}$ (P18510-1), IL-33$^{2-270}$ (O95760-1), IL-36α$^{6-158}$ (Q9UHA7-1), IL-36β1$^{5-164}$ (Q9NZH7-1), IL-36β2$^{5-157}$ (Q9NZH7-2), IL-36γ$^{18-169}$ (Q9NZH8-1), IL-36Ra$^{2-155}$ (Q9UBH0-1), IL-37$^{46-218}$ (Q9NZH6-1), IL-38-1$^{2-152}$ (Q8WWZ1-1), IL-38-2$^{2-152}$ (Q8WWZ1-2), caspase-4$^{105-377}$ (P49662-1) and optimized for *Escherichia coli* (*E. coli*) codon usage were cloned into G196/pcDNA3 [21] and used for human HEK-293 transfection. A synthetic gene coding for IL-18 was cloned into pcDNA3.

IL-18$^{37-193}$ was cloned into pET28-TEV [22] as a C-terminal His$_6$-tag, expressed in *E. coli*, purified using Ni-NTA agarose (QIAGEN, Valencia, CA, USA) and used for generation of mouse anti-human IL-18 mAbs as immunogen. N-terminal Met of the Met-IL-18$^{37-193}$-His was confirmed by Edman degradation sequencing.

IL-18 and caspase-4$^{105-377}$ were cloned into pET28-TEV, expressed in *E. coli* and purified using Ni-NTA agarose (QIAGEN) for making IL-18

neoepitope protein. A mixture of these proteins (IL-18:caspase-4$^{105-377}$ = 10:1) was incubated at 24 °C overnight and then run through a Ni-NTA agarose column. The flow-through was collected as IL-18 neoepitope protein (sFig. 1). The N-terminal Tyr of the IL-18 neoepitope was confirmed by Edman degradation sequencing.

This study was approved by the recombinant DNA experiment safety committee of Shimane University and carried out in accordance with the approved protocol (ID: 539-1).

2.4. mAb generation

Mouse anti-human IL-18 mAbs were generated by immunizing mice with a bacterially expressed fragment of human IL-18 protein (37–193) with an N-terminal His$_6$-tag. Mouse mAbs against the neoepitope of human IL-18 cleaved by caspase-1/4 were produced by immunizing mice with the neoepitope peptide YFGKLESK-C (mAbProtein) conjugated with keyhole-limpet hemocyanin (77666, Thermo Scientific). The sequence of the neoepitope peptide was ^{37}YFGKLESK^{44}, corresponding to the N-terminal end of cleaved IL-18, with an additional C-terminal Cys for conjugation. Serum titers were monitored by immunoblotting using HEK-293 cell lysate transfected with G196-IL-18$^{37-193}$/pcDNA3 for mouse anti-human IL-18 mAbs and with IL-18/pcDNA3 and G196-caspase-4$^{105-3}$/pcDNA3 for mouse mAbs against the neoepitope of human IL-18. Clonal populations of fusion cells were screened by ELISA for antibody production against His$_6$-tagged IL-18 protein (37–193) and the neoepitope peptide conjugated with BSA, respectively. Productive cells were cloned to monoclonal lines by serial dilution screening. Highly concentrated mAbs were isolated from murine ascites after intraperitoneal injection of the hybridoma cells. All animal experiments were performed in compliance with the standards established by the International Guiding Principles for Biomedical Research Involving Animals and were approved by the animal care and use committee of Shimane University (ID: IZ29-53).

2.5. Western blot analysis and immunoprecipitation

The samples were mixed with SDS buffer (125 mM Tris-HCl, pH 6.8, 5% glycerol, 4% SDS, 0.005% bromophenol blue, and 10% 2-mercaptoethanol), then subjected to 12% SDS-polyacrylamide gel electrophoresis and transferred onto a polyvinylidene difluoride membrane (Immobilon-P, IPVH00010, Merck Millipore, Darmstadt, Germany). After blocking with 5% nonfat dry milk for 30 min, the membranes were incubated with the indicated antibodies for 1 h at room temperature, followed by incubation with secondary antibodies (HRP-conjugated anti-mouse or anti-rabbit IgG at the appropriate dilutions) for 45 min at room temperature. Antibody binding was detected with an enhanced chemiluminescence detection system (PerkinElmer, Waltham, MA, USA). For quantitative analysis, images were acquired using an ImageQuant LAS 4000 (GE Healthcare, Buckinghamshire, England) and quantified using Multi Gauge software (Fujifilm, Tokyo, Japan).

Immunoprecipitation was conducted by pre-conjugating the antibodies with anti-mouse IgG agarose beads (A6531, Sigma-Aldrich).

2.6. Immunofluorescence microscopy

HeLa and HEK-293 cells were separately grown on glass coverslips coated with Type I-C Cellmatrix (Nitta Gelatin, Osaka, Japan). The cells were washed with PBS and fixed with PBS containing 3.7% formaldehyde for 20 min, then washed three times with PBS and permeabilized with PBS containing 1% Triton-X100 for 2 min. After washing with PBS, the cells were incubated with PBS containing 5% BSA for 30 min. After blocking, the cells were incubated with primary antibodies for 1 h at room temperature. After four washes with PBS, secondary antibody incubations were performed for 45 min at room temperature and the coverslips were mounted (mounting medium;

Vector Laboratories, Burlingame, CA, USA) with DAPI. Images were acquired using a confocal microscope (FV1000, Olympus, Tokyo, Japan).

2.7. Surface plasmon resonance analysis

Experiments were performed using a Biacore X100 (GE Healthcare, Uppsala, Sweden). The epitope peptides (the peptide sequences were QGNRPLFEDMTDSGSGS-C for mAb 11–4.1 and YFGKLESK-C for mAb 9–10.2; epitope sequences are underlined) were immobilized on a CM5 sensor chip (BR100012, GE Healthcare) via the thiol group of the added C-terminal Cys of the peptides using a thiol coupling kit (BR100557, GE Healthcare) according to the manufacturer's instructions. Five analyte concentrations (0.08, 0.4, 2, 10, and 50 nM for mAb 11–4.2, and 0.4, 2, 10, 50, and 250 nM for mAb 9–10.2) were used in the experiments. Single-cycle kinetic measurements were conducted at sequentially increasing analyte concentrations. Each kinetic assay was repeated at least three times. The data were analyzed using BIAevaluation software (GE Healthcare) assuming bivalency for the analyte.

2.8. Patients and samples

Serum samples were obtained from 14 patients with adult-onset Still's disease (AOSD), 6 patients with hemophagocytic syndrome, and patients with other inflammatory diseases such as pneumonia (n = 18), dermatomyositis (n = 18, including 7 anti-melanoma differentiation-associated gene 5 (anti-MDA5) antibody-positive patients), familial Mediterranean fever (n = 18, including 8 patients with fever attack) and Behcet's disease (n = 7) at Nagasaki University Hospital, Nagasaki Medical Center, and Fukushima Medical University in Japan. All patients underwent a clinical assessment and were diagnosed according to the criteria for each disease. All experiments were performed according to the Helsinki guidelines and the study protocol was approved by the research ethics committee of Shimane University, Nagasaki University Hospital, Nagasaki Medical Center, and Fukushima Medical University (ID: 20160511-1).

2.9. Capillary Western immunoassay (WES)

WES analysis was performed on a WES system (004–600, ProteinSimple, San Jose, CA, USA) according to the manufacturer's instructions using a 12–230 kDa separation module (SM-W004, ProteinSimple) and an anti-mouse detection module (DM-002, ProteinSimple). In brief, protein or serum samples were 10-fold diluted in sample buffer (100-fold diluted '10x Sample Buffer 2' from the Separation Module), then mixed with Fluorescent Master Mix and heated at 95 °C for 5 min. The samples, blocking reagent (antibody diluent), primary antibodies (in antibody diluent), HRP-conjugated secondary antibodies, and chemiluminescent substrate were pipetted onto the plate of the separation module. The instrument default settings used were: stacking and separation at 475 V for 30 min; blocking reagent for 5 min, primary and secondary antibody each for 30 min; and luminol/peroxide chemiluminescence detection for ~15 min (exposures of 1, -2, -4, -8, -16, −32, −64, −128 and −512 s). The resulting electropherograms were inspected to check whether the results of automatic peak detection required manual correction.

Differences in signals between experiments were controlled using a 5-point calibration curve of bacterially expressed and purified IL-18^{37-193} reference sample, typically in the ranging 2.5–40 ng/ml.

2.10. Epitope mapping

Epitope mapping of mAb 11–4.1 was achieved by preparing a series of fragments of human IL-18 by polymerase chain reaction (PCR) amplification using Pfu polymerase (02–021, BioAcademia) and IL-18 optimized for E. coli codon usage as the template. Alanine scanning

mutagenesis was conducted by generating all indicated short fragments of IL-18^{62-70} by annealing complementary oligos (Fasmac, Kanagawa, Japan). The amplified fragments and the annealed oligos were cloned into the pGEX4T-2 vector (GE Healthcare). The final constructs were sequenced to ensure that no mutations had occurred during the PCR and cloning processes. BL21 (DE3) E. coli cells were transformed with the plasmids, and protein expression was induced with 0.1 mM isopropyl-β-D-1-thiogalactopyranoside (IPTG).

Epitope mapping of neoepitope mAb 9–10.2 was achieved by substituting individually each position of the neoepitope peptide YFGKL-ESK-C with Ala (mAbProtein). These neoepitope peptides were conjugated with BSA (77667, Thermo Scientific) and subjected to ELISA.

2.11. Statistical analysis

Protein concentration values evaluated by ELISA for samples in which the same protein was detectable with WES (WES, n = 19) and undetectable (NA in WES, n = 22) were plotted with the generic "plot" function of GNU R (http://www.r-project.org, version 3.3.3).

Protein concentration values evaluated by ELISA and WES; and by WES with mAbs 9–10.2 and 11–4.1 were plotted with the "plot" function of GNU R. A line of slope 1, with the intercept at 0, was drawn with the "abline" function. Pearson's correlation test was performed using the "cor.test" function. For Fig. 2C, we removed the two outlier samples with the first and second highest WES values.

2.12. IFN-γ induction assay

Human IL-18 proteins were examined for the ability to induce IFN-γ production from KG-1 human acute myeloblastic leukemia cells at 37 °C (Fig. 4A) as described previously [23].

2.13. Enzyme-linked immunosorbent assay (ELISA)

Serum concentrations of IL-18 and supernatant concentrations of IFN-γ from KG-1 cells were measured by enzyme-linked immunosorbent assay (ELISA) using a human IL-18 ELISA kit (7620, MBL, Nagoya, Japan) and a human IFN-γ ELISA kit (851.560.005, Diaclone, Cedex, France), respectively.

2.14. Molecular imaging

Molecules were rendered from images using PyMOL software (Schrödinger, New York, NY, USA). We applied the coordinates and structure factors for the surface models of human IL-18 (Protein Data Bank (PDB) code, 1J0S), IL-18 and IL-18Ra (PDB code, 3WO4), IL-18 and ectromelia virus IL-18BP (PDB code, 3F62), and L-18 and yaba-like disease virus IL-18BP (PDB code, 4EEE).

3. Results

3.1. Novel mAbs against human IL-18

We raised monoclonal antibodies (mAbs) against human IL-18 by immunizing mice with a bacterially expressed fragment of human IL-18 protein (37–193) and established the hybridoma clones 11–4.1, 4–18.1 and 9–4.2 (Fig. 1A). The IL-18^{37-193} signal detected by capillary Western immunoassay (WES) was consistent with a molecular weight of approximately 24 kDa, which is higher than the predicted molecular weight of 18 kDa. This size discrepancy can be explained by the molecular weight ladder used in WES, which overestimates molecular weights below 25 kDa (Data not shown). Similar discrepancy has also been reported [24]. The specificity of IL-18 detection by WES was confirmed by several antibodies against IL-18 (which recognize different IL-18 epitopes) all providing the same signal at 24 kDa (Fig. 5A, sFig. 2, sFig. 3A and B).
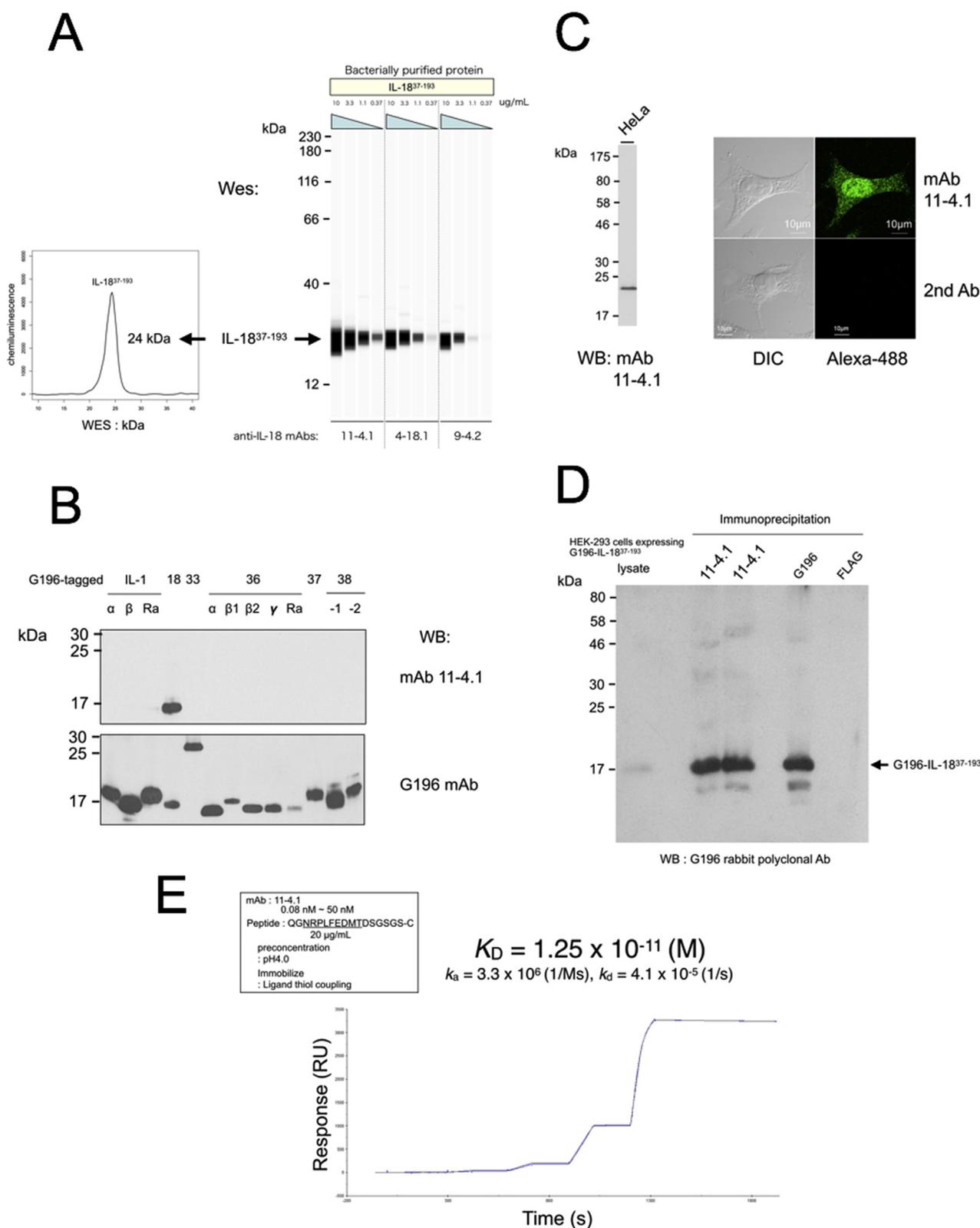
Fig. 1. Characterization of anti-human IL-18 mAbs.
(A) Capillary Western immunoassay (WES) of serial dilutions of bacterially purified IL-18 protein cleaved by caspase-4 (IL-18$^{37-193}$) with the newly generated mAbs. The IL-18$^{37-193}$ signal with a molecular weight of approximately 24 kDa detected by capillary WES was higher than the predicted molecular weight of 18 kDa. (B) Specificity of mAb 11–4.1. The mAb selectively recognized human IL-18 from HEK-293 cell lysates expressing IL-1 family proteins by Western blot (WB) analysis. (C) WB (left panel) and immunofluorescence (right panel) analysis of endogenous IL-18 from HeLa cells with mAb 11–4.1. DIC, differential interference contrast. Alexa-488, compressed confocal z-stack of Alexa-488 immunofluorescence. Bar = 10 μm. (D) Immunoprecipitation of HEK-293 cell lysate transfected with G196-tagged IL-18$^{37-193}$ with mAb 11–4.1. G196, positive control mAb; FLAG, negative control mAb. (E) A representative binding sensorgram for the interaction between mAb 11–4.1 and the epitope peptide using the single-cycle kinetic assay format. The peptide was first captured on a CM5 sensor chip using thiol coupling, then five concentrations of mAb 11–4.1 were injected.
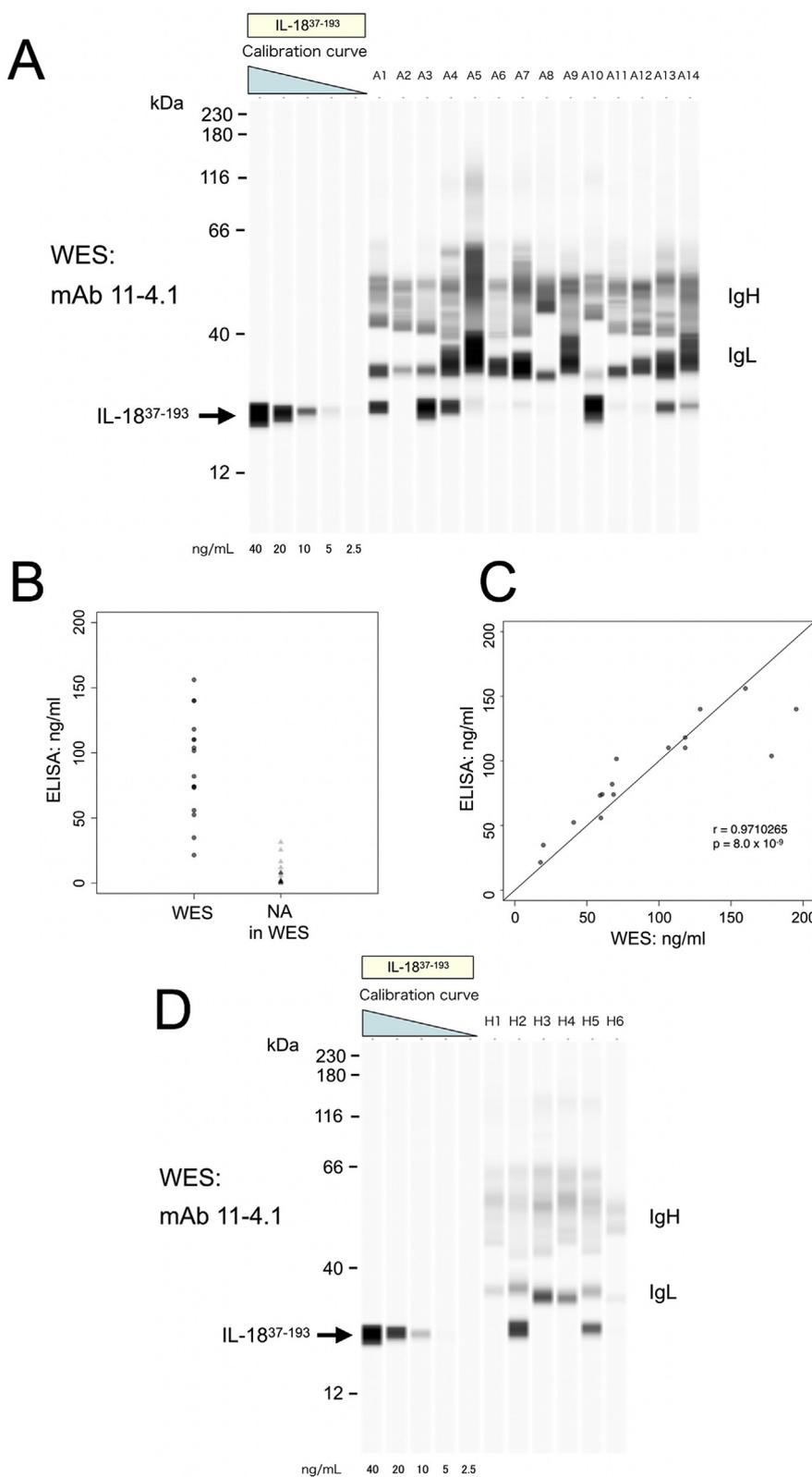
Fig. 2. Detection of endogenous IL-18 from the serum of inflammatory patients using WES and mAb 11–4.1. (A) WES analysis of the serum of adult-onset Still's disease (AOSD) patients using mAb 11–4.1. IgH, heavy chain of immunoglobulin; IgL, light chain of immunoglobulin. (B) Dot plot of the protein concentrations determined by ELISA in serum from AOSD patients in which the same protein was detectable using WES (WES, n = 19) or was undetectable (NA in WES, n = 22). (C) Dot plot of the protein concentration determined by ELISA and Wes were plotted with the "plot" function of R. A line of slope 1, with the intercept at 0, was drawn with the "abline" function. r, Pearson's product-moment correlation coefficient. (D) WES analysis of the serum of hemophagocytic syndrome patients using mAb 11–4.1. IgH, heavy chain of immunoglobulin; IgL, light chain of immunoglobulin.

These antibodies selectively recognized human IL-18 from HEK-293 cell lysates expressing IL-1 family proteins (Fig. 1B and sFig. 4). mAb 11–4.1 detected endogenous IL-18 from HeLa cells as a full-length protein by Western blot analysis (Fig. 1C, left panel), and a fine granular pattern was observed throughout the cell, including the nucleus, by immunofluorescence analysis (Fig. 1C, right panel). The nuclear localization signal (NLS) prediction program cNLS Mapper (http://nls-mapper.iab.keio.ac.jp/cgi-bin/NLS_Mapper_form.cgi) indicated no NLS in human IL-18, demonstrating that nuclear pore complexes allow passive diffusion of IL-18 (< 50 kDa) into the nucleus [25]. mAb 11–4.1 was suitable for immunoprecipitation (Fig. 1D). The bivalent analyte model (provided by the Biacore evaluation software) was fitted to the surface plasmon resonance experimental data and provided an estimate for K_D of 1.25×10^{-11} M (Fig. 1E).

Fig. 3. Precise epitope mapping of mAb 11–4.1.

(A) Single alanine replacement analysis of the candidate epitope ^{62}NRPLFEDMT^{70} fused with N-terminal GST protein using mAb 11–4.1 (upper panel) and G196 (lower panel) of the bacterially expressed proteins. The GST fusion proteins contained the epitope DLVPR of mAb G196. The mean values of the images acquired using an ImageQuant LAS 4000 are shown (n = 3). (B) Epitope mapping on human IL-18 Molecules were rendered from images using PyMOL software. Left panel, IL-18 (grey, PDB code, 3F62); right panel, IL-18 (grey) and IL-18Rα (green) (PDB code, 3WO4). The epitope on IL-18 molecule was colored in pink and orange. Alanine substitution of the residues colored in pink had the most profound effect in Fig. 3A.

3.2. Endogenous IL-18 detection in the serum of inflammatory patients by WES analysis with mAb 11–4.1

Serum IL-18 levels in healthy human subjects are in the range 36–260 pg/ml, as determined using a commercial ELISA kit (IL-18 ELISA Kit 7620; MBL, Nagoya, Japan, https://www.mblintl.com/assets/7620_110801_.pdf). This range is below the limit of detection by Western blotting. In contrast, the serum levels of IL-18 were particularly high in adult-onset Still's disease (AOSD) patients [26–29] (over 1000 times that in healthy controls [30–39]. Having shown that mAb

11–4.1 binds with high affinity and specificity to IL-18, we conducted WES analysis of serum from patients with AOSD. IL-18 bands in 6 (43%) of 14 AOSD samples were clearly visible and, importantly, had a molecular weight corresponding to IL-18$^{37-193}$ (Fig. 2A).

Next, we subjected the 41 AOSD samples in which we measured the serum concentration of IL-18 by ELISA to WES analysis. IL-18 bands were visible for 100% of the patients with an IL-18 concentration above 50 ng/ml as measured by ELISA (n = 17) and for half of the patients with IL-18 concentrations in the range 20–35 ng/ml (n = 4); in contrast, no bands were visible for 100% of the patients with IL-18 levels
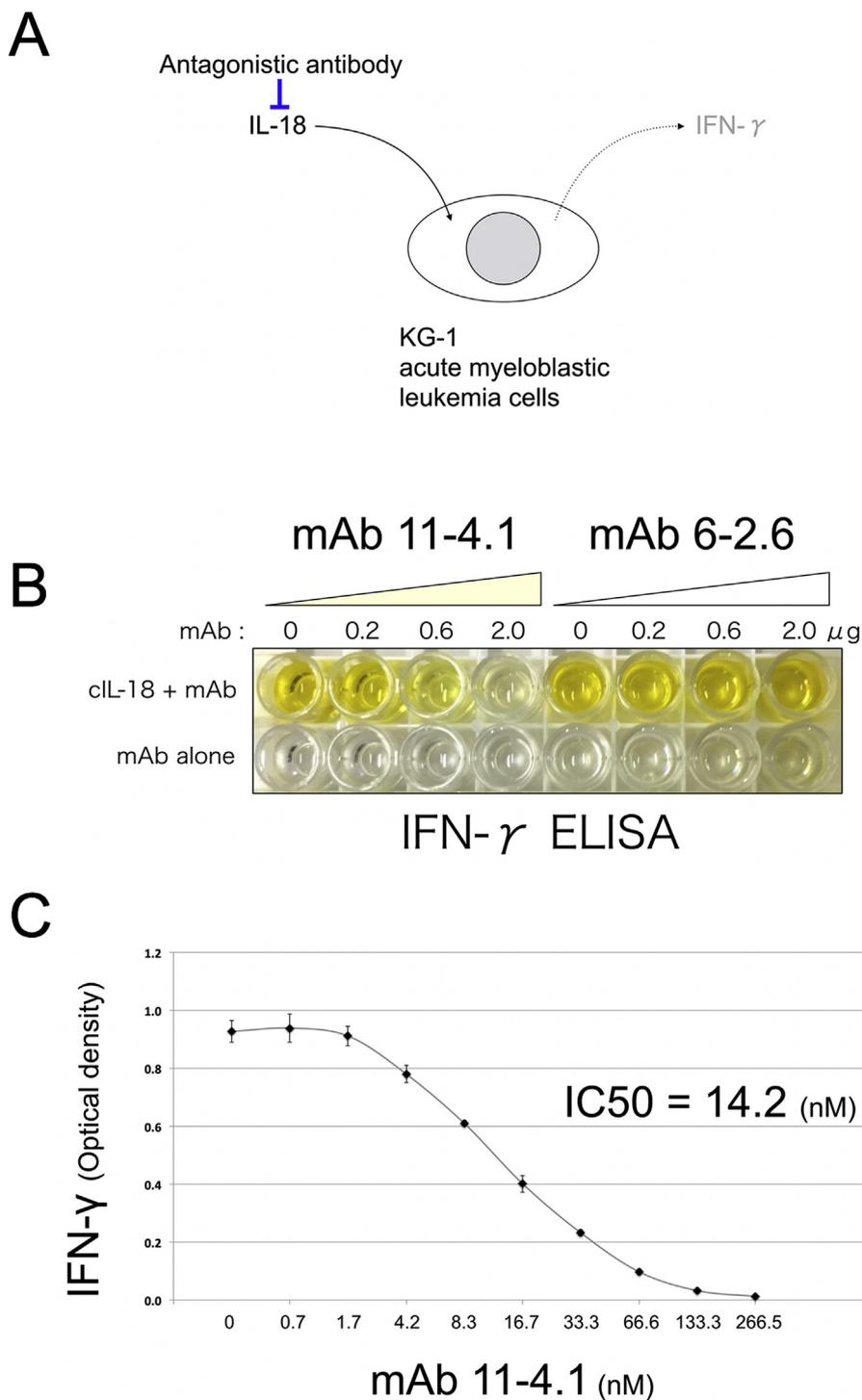
Fig. 4. Function inhibition assay of IL-18 by mAb 11–4.1.
(A) Outline of the experiment. (B) ELISA detection of IL-18-evoked IFN-γ release with serial dilutions of mAbs 11–4.1 and 6–2.6 from KG-1 cells. Anti-IL-18 mAb 6–2.6 recognized the epitope 128–142 of human IL-18, which did not overlap with IL-18/IL-18 receptor binding. (C) The mean and standard deviation of three independent ELISA experiments are shown.

below 20 ng/mL as measured by ELISA (n = 20) (Fig. 2B). We used the AOSD sample in which IL-18 was detected as a visible band (n = 17) by WES and performed a correlation analysis of the IL-18 values determined using WES and ELISA. The analysis revealed a positive correlation between the values measured by both techniques (correlation coefficient: 0.97), which is statistically significant (p = 8.0×10^{-9}) (Fig. 2C).

We investigated the IL-18 serum levels of 6 patients with

hemophagocytic syndrome and patients with other inflammatory diseases such as pneumonia (n = 18), dermatomyositis (n = 18, including 7 anti-MDA5 antibody-positive patients), familial Mediterranean fever (n = 18, including 8 patients with fever attack) and Behcet's disease (n = 7). An IL-18 signal corresponding to IL-18$^{37-193}$ was clearly visible for 2 (33%) of the 6 hemophagocytic syndrome patients (Fig. 2D), whereas no bands were visible for the other patients (data not shown).
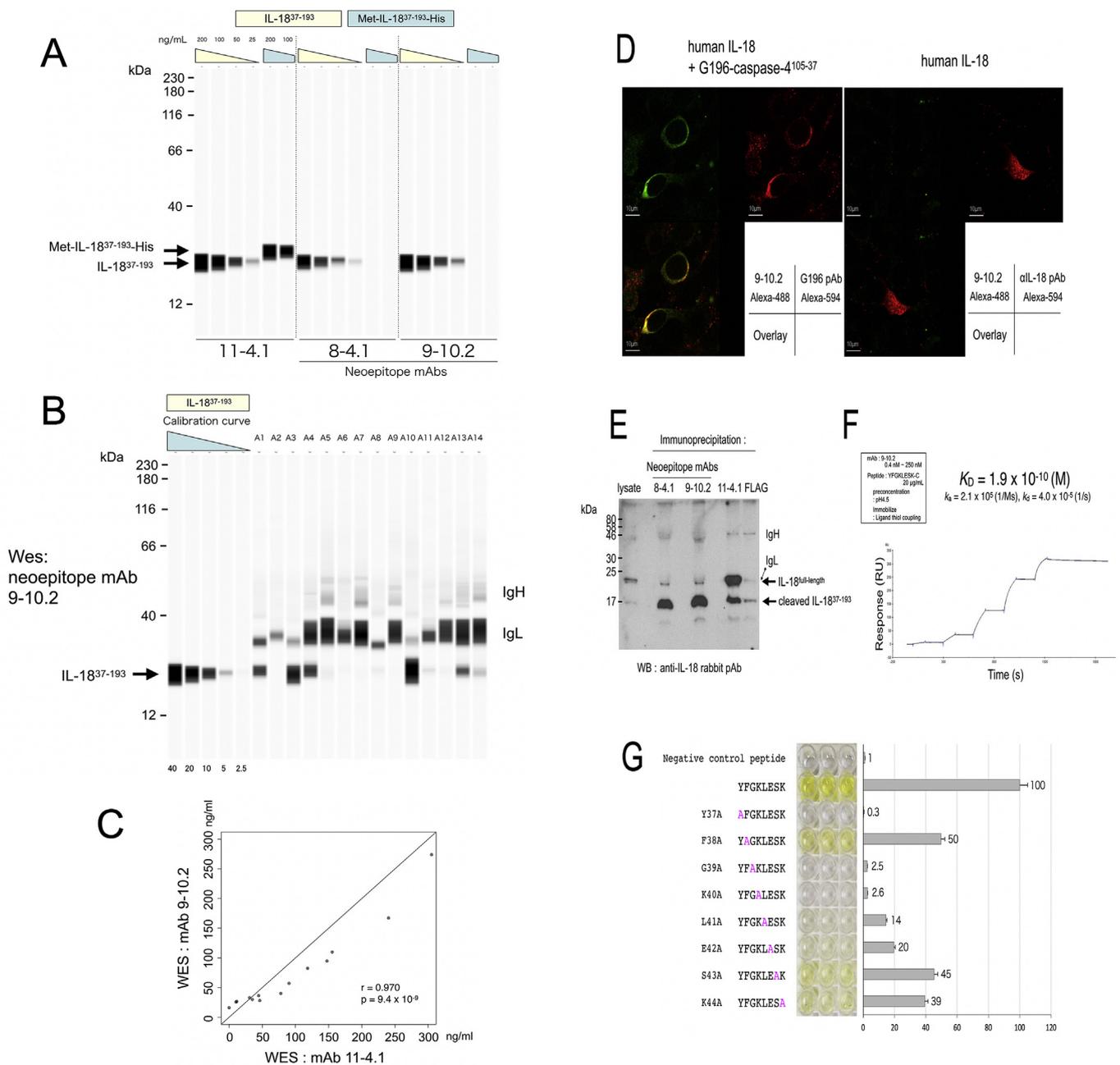
Fig. 5. Characterization of novel mAbs against the neoepitope of human IL-18 cleaved by inflammatory caspase-1/4.
(A) Capillary Western immunoassay (WES) of serial dilutions of bacterially purified IL-18 protein cleaved by caspase-4 (IL-18$^{37-193}$) and Met-IL-18$^{37-193}$ with the newly generated neoepitope mAbs. IgH, heavy chain of immunoglobulin; IgL, light chain of immunoglobulin. (B) WES analysis of serum of adult-onset Still's disease (AOSD) patients with mAb 9–10.2. The serum samples were the same as used to obtain the data shown in Fig. 2A. IgH, heavy chain of immunoglobulin; IgL, light chain of immunoglobulin. (C) Dot plot of the protein concentration determined by Wes analysis with mAbs 9–10.2 and 11–4.1 were plotted with the "plot" function of R. A line of slope 1, with the intercept at 0, was drawn with the "abline" function. r, Pearson's product-moment correlation coefficient. (D) Immunofluorescence analysis of HEK-293-expressed full-length IL-18 and G196-tagged activated caspase-4$^{105-307}$ (left panel) or HEK-293-expressed full-length IL-18 alone (right panel) with neoepitope mAb 9–10.2 and the indicated polyclonal Ab. Each image was a confocal z-stack image. Bar = 10 μm. (E) Immunoprecipitation of HEK-293 cells lysate transfected with full-length IL-18 and G196-tagged activated caspase-4$^{105-307}$ with neoepitope mAbs 8–4.1 and 9–10.2. 11–4.1, mAb against IL-18$^{62-68}$. FLAG, negative control mAb. (F) A representative binding sensorgram for the interaction between mAb 9–10.2 and the neoepitope peptide using the single-cycle kinetic assay format. The peptide was first captured on a CM5 sensor chip using thiol coupling, then five concentrations of mAb 9–10.2 were injected. (G) Precise epitope mapping of mAb 9–10.2 using ELISA. Each position of the neoepitope peptide YFGKLESK-C was substituted individually with Ala. The mean and standard deviation of three independent ELISA experiments are shown as 100% of the mean value of wild type peptide (right panel). (H) Epitope mapping of mAb 9–10.2 on human IL-18. Molecules were rendered from images using PyMOL software. Left panel, IL-18 (grey, PDB code, 1J0S); right panel, IL-18 (grey) and IL-18Ra (green) (PDB code, 3WO4). The epitope of neoepitope mAb 9–10.2 on IL-18 molecule was colored in pink and orange. Alanine substitution of the residues colored in pink had the most profound effect in Fig. 5G. (I) Function inhibition assay of IL-18 using mAb 9–10.2. The mean and standard deviation of three independent ELISA experiments are shown. (J) Relationship between IL-18, IL-18BP, and the epitope of neoepitope mAb 9–10.2. Molecules were rendered from images using PyMOL software. Left panel, IL-18 (grey, PDB code, 1J0S); middle panel, IL-18 (grey) and ectromelia virus IL-18BP (blue) (PDB code, 3F62); right panel, IL-18 (grey) and yaba-like disease virus IL-18BP (blue) (PDB code, 4EEE). The epitope on IL-18 molecule was colored in pink and orange. The color code is the same as in (H). (K) Summary of the newly generated mAbs.
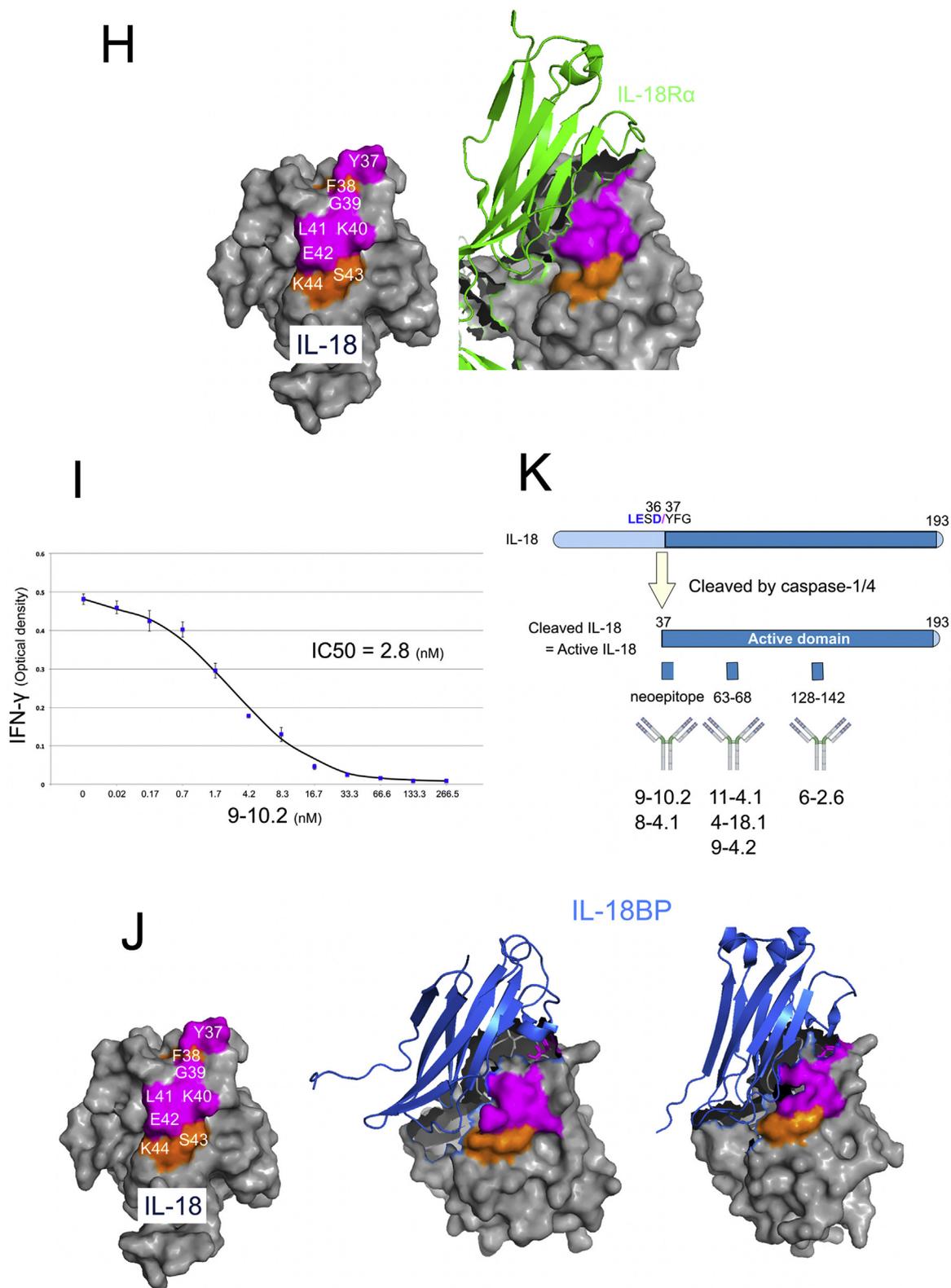
Fig. 5. (*continued*)

3.3. Determination of precise epitope recognized by mAb 11–4.1

We mapped the epitope recognized by mAb 11–4.1 by subjecting a series of bacterially expressed GST-tagged truncated mutants of human IL-18 to Western blot analysis (sFig. 5) and identified amino acid residues 62–70 as the minimal epitope recognized by the mAb (sFig. 5, right panel).

We then performed alanine scanning mutagenesis on the epitope to determine which amino acid residues are responsible for mAb recognition (Fig. 3A). The D68A (Asp to Ala at residue 68) and R63A substitutions had the most profound effects, reducing the detection levels by 95% and 80%, respectively (Fig. 3A, lanes 8 and 3, compared

with lane 1). The L65A, F66A, and E67A substitutions had much milder, although statistically significant, effects (30% reduction on average). In contrast, the N62A, P64A, M69A and T70A mutants of IL-18 (62–70) were detected by mAb 11–4.1, comparable to that of the wild type. These results clarified that the six amino acid residues 63-RPLFED-68 are the epitope of mAb 11–4.1, and that the epitope contains two critical charged amino acids (Asp68 and Arg63) and one nonessential residue (Pro 64).

We mapped the epitope on human IL-18. The epitope was located on the surface of the IL-18 molecule (Fig. 3B, *left panel*) as expected, and the mapping showed that the epitope overlaps with IL-18/IL-18 receptor binding (Fig. 3B, *right panel*).

3.4. Inhibition of IL-18-induced IFN-γ release in KG-1 cells by mAb 11–4.1

Human IL-18 induced IFN-γ release from KG-1 human acute myeloblastic leukemia cells in a dose-dependent manner (Fig. 4A) [23]. IL-18-evoked IFN-γ release was blocked dose-dependently by mAb 11–4.1, with an estimated IC50 value of 14.2 nM (Fig. 4B and C). Furthermore, we developed another anti-IL-18 mAb named 6–2.6, which recognizes another epitope (128–142) of human IL-18 and does not overlap with IL-18/IL-18 receptor binding (data not shown). As expected, mAb 6–2.6 did not inhibit IL-18-induced IFN-γ release from KG-1 cells (Fig. 4B), providing the specificity of inhibition by mAb 11–4.1.

3.5. Novel mAbs against the neoepitope of human IL-18 generated through inflammasome activation

Activated pro-inflammatory caspases, such as caspase-1 (in human and mouse), and caspase-4 (in human) or caspase-11 (in mouse), cleave and activate the pro-inflammatory cytokines IL-1β and IL-18 [5,6]. Once cleaved through inflammasome activation, the N-terminus of active IL-18 represents a novel epitope not present in normal cells. Therefore, detection of this neoepitope could be a unique and sensitive indicator of inflammatory action. We therefore raised mAbs against the neoepitope of human IL-18 by immunizing mice with the neoepitope peptide corresponding to the N-terminal end of cleaved IL-18.

We established two hybridoma clones, 8–4.1 and 9–10.2, which selectively recognized the neoepitope of bacterially expressed IL-18 cleaved by caspase-4, but not a bacterially expressed fragment of human IL-18 protein (37–193) tagged with a C-terminal His_6 (Fig. 5A). This lack of recognition was attributed to the N-terminal Met of IL-18^{37-193}, which was not removed by methionyl aminopeptidase due to the large side-chain of the penultimate amino acid, Y37 [40,41]. The N-terminal Tyr of IL-18 cleaved by caspase-4 and the N-terminal Met of IL-18^{37-193} were confirmed by Edman degradation sequencing (data not shown). As expected, mAb 11–4.1 recognized both proteins (Fig. 5A).

Neoepitope mAb 9–10.2 recognized IL-18 cleaved by caspase-4 with an affinity comparable to that of mAb 11–4.1. We therefore used neoepitope mAb 9–10.2 to perform WES analysis of the same AOSD patient sera as used to provide the data shown in Fig. 2A. The neoepitope signals obtained with mAb 9–10.2 were approximately equivalent to the IL-18 signals obtained with mAb 11–4.1 (Fig. 5B, compare to Fig. 2A). Correlation analysis revealed a positive correlation between the values measured using mAb 9–10.2 and mAb 11–4.1 (correlation coefficient: 0.970), which is statistically significant (p = 9.4×10^{-9}). mAb 9–10.2 was also appropriate for immunostaining (Fig. 5D) and immunoprecipitation (Fig. 5E). The bivalent analyte model was fitted to the surface plasmon resonance experimental data and provided an estimated K_D value of 1.9×10^{-10} M (Fig. 5F).

We performed alanine scanning mutagenesis on the neoepitope peptide to determine which amino acid residues of the neoepitope were responsible for mAb recognition (Fig. 5G). The single substitutions Y37A, G39A and K40A resulted in the most profound effects, reducing detection levels by more than 95%. The L41A and E42A substitutions had much milder effects (more than 80% reduction), and the F38A,

S43A and K44A substitutions had even less pronounced effects (around 50–60% reduction). These results clarified that the eight amino acid residues ^{37}YFGKLESK^{44} are the epitope of mAb 9–10.2 and that Y37, G39 and K40 of the neoepitope are critical for recognition by mAb 9–10.2.

We mapped the epitope of neoepitope mAb 9–10.2 on human IL-18. The epitope was located on the surface of the IL-18 molecule (Fig. 5H, *left panel*), and the mapping showed that the epitope overlaps with IL-18/IL-18 receptor binding (Fig. 5H, *right panel*). As expected, mAb 9–10.2 diminished IL-18-induced IFN-γ release effectively and dose-dependently, with an estimated IC50 value of 2.8 nM (Fig. 5I).

4. Discussion

Here we described the characterization of two types of mAbs against human IL-18 which exhibit defined properties. The mAbs were characterized using Western blotting, capillary Western immunoassay (WES), immunofluorescence, immunoprecipitation, surface plasmon resonance analysis, epitope mapping, and function-blocking assays. The innovative aspect of these mAbs lies in the exact molecular weight determination of serum IL-18 in adult-onset Still's disease (AOSD) and hemophagocytic syndrome patients, with specificity and high affinity. The application of WES to these mAbs allowed visualization of the IL-18 bands and provided a molecular weight corresponding to the pro-inflammatory caspase-1/4 cleaved, active form IL-18^{37-193}, and not to the inactive precursor IL-18, in the serum of AOSD and hemophagocytic syndrome patients. Likewise, only cleaved IL-18 in the serum of AOSD patients was detected with polyclonal anti-IL-18 antibody [31]. This polyclonal antibody is currently not commercially available.

Western blotting is a very commonly used technique in molecular biology. However, the analysis of serum from patients using Western blotting is time-consuming, and the target protein bands are usually irregular and reproducibility is poor, thereby providing largely qualitative data. This has been addressed recently by the development of next generation Western blotting techniques such as capillary Western immunoassay (WES). WES is a gel- and blot-free automated, quantitative method that requires less sample and less time than a conventional Western blot assay. We demonstrate here that two types of mAbs against human IL-18 are suitable for the WES analysis of serum from patients with inflammatory diseases (Figs. 2A and 5B), offering novel possibilities for increasing the clinical implications between IL-18 and inflammatory diseases.

Eleven members of the IL-1 family are intracellular molecules; the only known exception is an IL-1 receptor antagonist (IL-1Ra; also known as IL-1RN) possessing an N-terminal signal peptide, similar to that of most cytokines, including interferons and interleukins [42]. As described in the Introduction, proteolysis of the IL-18 precursor into the mature, active molecule is dependent on pro-inflammatory caspase-1/4, but exceptions exist [1,3,13,43]. For example, it was reported that IL-18 precursor is released from dying cells and processed extracellularly, most likely by neutrophil proteases such as leukocyte proteinase-3 (PR3; also known as neutrophil proteinase 4, NP-4, myeloblastin) [44]. Such processing is possible because the leukocyte count is a marker of inflammation widely used in clinical practice. Four cardinal symptoms of AOSD are traditionally characterized, of which one is increased leukocyte and neutrophil counts [27–29]. As shown in Fig. 5C, the values estimated using neoepitope mAb 9–10.2 (value$_{9-10.2}$) correlated well with that estimated using mAb 11–4.1 (value$_{11-4.1}$) (r = 0.970, p < 0.01, n = 14), but value$_{9-10.2}$ was generally much smaller than value$_{11-4.1}$ above 50 ng/ml. Given that PR3 prefers small aliphatic amino acids (Ala, Ser and Val) at the P1 site [45], the IL-18 neoepitope generated by PR3 differs form that generated by caspase-1/4 (which strictly requires a negatively charged Asp at position P1). Therefore, neoepitope mAb 9–10.2 could not recognize the neoepitope generated by PR3. Taken together, it is possible that the difference between value$_{9-10.2}$ and value$_{11-4.1}$ is due to IL-18 being cleaved by different

proteases such as PR3. In the future we will raise neoepitope mAbs cleaved by PR3 to detect IL-18 cleaved by PR3 in the sera of patients with inflammatory diseases.

Immunofluorescence analysis revealed that endogenous IL-18 localized throughout the cell including the nucleus in HeLa cells (Fig. 1C), whereas overexpressed IL-18 almost exclusively localized in the cytoplasm (Fig. 5 and sFig. 6). The differences are probably because of formation of intermolecular disulfide bonds among the cysteine residues of IL-18 [46,47]. Given that the molecular size of oligomerized IL-18 is much larger than the diffusion limit ($\sim 50\,kDa$) of the nuclear pore complex [25], the overexpressed protein is prone to form oligomers and could not enter the nucleus.

Western blot and WES analyses have detection limits, even when using high affinity antibodies, although mAb 11–4.1 could detect purified IL-18 protein above 10 ng/ml, which results in a loading amount of 0.05 ng (Fig. 2A, calibration curve). WES analysis using mAb 11–4.1 of patient' sera below 20 ng/ml IL-18 as measured by ELISA analysis was unsuccessful in visualizing IL-18 bands (Fig. 2B). Thus, concentrations below 20 ng/ml IL-18 require a highly sensitive, reproducible and quantitative ELISA system. A naturally occurring IL-18 binding protein (IL-18BP) blocks IL-18 signaling by binding to IL-18 like a decoy receptor, similar to poxvirus IL-18BPs [3,13,48,49]. The molecular structures of IL-18, IL-18BP, and the epitope of neoepitope mAb 9–10.2 show that the epitope of neoepitope mAb 9–10.2 overlaps with IL-18/IL-18BP binding (Fig. 5J), implying that neoepitope mAb 9–10.2 cannot bind to the IL-18/IL-18BP complex. A refined ELISA detection system for mature, active, free IL-18 from IL-18BP could be developed by utilizing neoepitope mAb 9–10.2 in combination with epitope-different mAbs, such as 11–4.1 and 6–2.6 (Fig. 5K). Such a system might be useful in inflammasome biology, and for diagnostic and therapeutic strategies for inflammatory diseases.

Conflicts of interest

YN, HK (Hiroki Kamino), EO and TU are co-inventors on the patent application related to the mAbs against IL-18 described in this paper. TU is employed by Shimane University and is currently co-founder and Chief Medical & Scientific Officer of mAbProtein, a biotech company focusing on the development and commercial utilization of mAbs for inflammation research, diagnosis and treatment. All other authors have declared no conflicts of interest. The potential conflict of interest by TU does not alter the authors' adherence to all the Archives of Biochemistry and Biophysics policies on sharing data and materials, as detailed online in the guide for authors.

Author contributions

Conceived and designed the experiments: TU. Performed the experiments: YN, HK, EO, HK, TS, TU, KM, TK, and AK. Performed surface plasmon resonance experiments and analysis: TU, KS, KK, MK, and KT. Analyzed the data: YN, HK, EO, HK, TS, TU, KM, TK, AK and KS. Wrote the paper: YN and TU. All authors contributed to the preparation and writing of the manuscript.

Acknowledgments

Appendix A. Supplementary data

Supplementary data to this article can be found online at https://doi.org/10.1016/j.abb.2019.01.001.

References

[1] K. Nakanishi, T. Yoshimoto, H. Tsutsui, H. Okamura, Interleukin-18 regulates both Th1 and Th2 responses, Annu. Rev. Immunol. 19 (2001) 423–474 https://doi.org/10.1146/annurev.immunol.19.1.423.

[2] C.A. Dinarello, Immunological and inflammatory functions of the interleukin-1 family, Annu. Rev. Immunol. 27 (2009) 519–550 https://doi.org/10.1146/annurev.immunol.021908.132612.

[3] C. Garlanda, C.A. Dinarello, A. Mantovani, The interleukin-1 family: back to the future, Immunity 39 (2013) 1003–1018 https://doi.org/10.1016/j.immuni.2013.11.010.

[4] K. Schroder, J. Tschopp, The inflammasomes, Cell 140 (2010) 821-632 https://doi.org/10.1016/j.cell.2010.01.040.

[5] D.E. Place, T.D. Kanneganti, Recent advances in inflammasome biology, Curr. Opin. Immunol. 50 (2018) 32–38 https://doi.org/10.1016/j.coi.2017.10.011.

[6] F. Awad, E. Assrawi, C. Louvrier, C. Jumeau, S. Georgin-Lavialle, G. Grateau, S. Amselem, I. Giurgea, S.A. Karabina, Inflammasome biology, molecular pathology and therapeutic implications, Pharmacol. Ther. 187 (2018) 133–149 https://doi.org/10.1016/j.pharmthera.2018.02.011.

[7] J. Shi, Y. Zhao, K. Wang, X. Shi, Y. Wang, H. Huang, Y. Zhuang, T. Cai, F. Wang, F. Shao, Cleavage of GSDMD by inflammatory caspases determines pyroptotic cell death, Nature 526 (2015) 660–665 https://doi.org/10.1038/nature15514.

[8] N. Kayagaki, I.B. Stowe, B.L. Lee, K. O'Rourke, K. Anderson, S. Warming, T. Cuellar, B. Haley, M. Roose-Girma, Q.T. Phung, P.S. Liu, J.R. Lill, H. Li, J. Wu, S. Kummerfeld, J. Zhang, W.P. Lee, S.J. Snipas, G.S. Salvesen, L.X. Morris, L. Fitzgerald, Y. Zhang, E.M. Bertram, C.C. Goodnow, V.M. Dixit, Caspase-11 cleaves gasdermin D for non-canonical inflammasome signalling, Nature 526 (2015) 666–671 https://doi.org/10.1038/nature15541.

[9] S. Feng, D. Fox, S.M. Man, Mechanisms of Gasdermin Family Members in Inflammasome Signaling and Cell Death, J. Mol. Biol. 430 (2018) 3068–3080 https://doi.org/10.1016/j.jmb.2018.07.002.

[10] N. Tsutsumi, T. Kimura, K. Arita, M. Ariyoshi, H. Ohnishi, T. Yamamoto, X. Zuo, K. Maenaka, E.Y. Park, N. Kondo, M. Shirakawa, H. Tochio, Z. Kato, The structural basis for receptor recognition of human interleukin-18, Nat. Commun. 5 (2014) 5340 https://doi.org/10.1038/ncomms6340.

[11] H. Wei, D. Wang, Y. Qian, X. Liu, S. Fan, H.S. Yin, X. Wang, Structural basis for the specific recognition of IL-18 by its alpha receptor, FEBS Lett. 588 (2014) 3838–3843 https://doi.org/10.1016/j.febslet.2014.09.019.

[12] S. Alboni, D. Cervia, S. Sugama, B. Conti, Interleukin 18 in the CNS, J. Neuroinflammation 7 (2010) 9 https://doi.org/10.1186/1742-2094-7-9.

[13] C.A. Dinarello, D. Novick, S. Kim, G. Kaplanski, Interleukin-18 and IL-18 binding protein, Front. Immunol. 4 (2013) 289 https://doi.org/10.3389/fimmu.2013.00289.

[14] E.S. Weiss, C. Girard-Guyonvarc'h, D. Holzinger, A.A. de Jesus, Z. Tariq, J. Picarsic, E.J. Schiffrin, D. Foell, A.A. Grom, S. Ammann, S. Ehl, T. Hoshino, R. Goldbach-Mansky, C. Gabay, S.W. Canna, Interleukin-18 diagnostically distinguishes and pathogenically promotes human and murine macrophage activation syndrome, Blood 131 (2018) 1442–1455 https://doi.org/10.1182/blood-2017-12-820852.

[15] N. Romberg, K. Al Moussawi, C. Nelson-Williams, A.L. Stiegler, E. Loring, M. Choi, J. Overton, E. Meffre, M.K. Khokha, A.J. Huttner, B. West, N.A. Podoltsev, T.J. Boggon, B.I. Kazmierczak, R.P. Lifton, Mutation of NLRC4 causes a syndrome of enterocolitis and autoinflammation, Nat. Genet. 46 (2014) 1135–1139 https://doi.org/10.1038/ng.3066.

[16] S.W. Canna, A.A. de Jesus, S. Gouni, S.R. Brooks, B. Marrero, Y. Liu, M.A. DiMattia, K.J. Zaal, G.A. Sanchez, H. Kim, D. Chapelle, N. Plass, Y. Huang, A.V. Villarino, A. Biancotto, T.A. Fleisher, J.A. Duncan, J.J. O'Shea, S. Benseler, A. Grom, Z. Deng, R.M. Laxer, R. Goldbach-Mansky, An activating NLRC4 inflammasome mutation causes autoinflammation with recurrent macrophage activation syndrome, Nat. Genet. 46 (2014) 1140–1146 https://doi.org/10.1038/ng.3089.

[17] A. Kitamura, Y. Sasaki, T. Abe, H. Kano, K. Yasutomo, An inherited mutation in NLRC4 causes autoinflammation in human and mice, J. Exp. Med. 211 (2014) 2385–2396 https://doi.org/10.1084/jem.20141091.

[18] Y. Kawasaki, H. Oda, J. Ito, A. Niwa, T. Tanaka, A. Hijikata, R. Seki, A. Nagahashi, M. Osawa, I. Asaka, A. Watanabe, S. Nishimata, T. Shirai, H. Kawashima, O. Ohara, T. Nakahata, R. Nishikomori, T. Heike, M.K. Saito, Identification of a High-Frequency Somatic NLRC4 Mutation as a Cause of Autoinflammation by Pluripotent Cell-Based Phenotype Dissection, Arthritis Rheum. 69 (2017) 447–459 https://doi.org/10.1002/art.39960.

[19] J. Barsalou, A. Blincoe, I. Fernandez, D. Dal-Soglio, L. Marchitto, S. Selleri, E. Haddad, A. Benyoucef, F. Touzot, Rapamycin as an Adjunctive Therapy for NLRC4 Associated Macrophage Activation Syndrome, Front. Immunol. 9 (2018) 2162 https://doi.org/10.3389/fimmu.2018.02162.

[20] N. Romberg, T.P. Vogel, S.W. Canna, NLRC4 inflammasomopathies, Curr. Opin. Allergy Clin. Immunol. 17 (2017) 398–404 https://doi.org/10.1097/aci.0000000000000396.

[21] K. Tatsumi, G. Sakashita, Y. Nariai, K. Okazaki, H. Kato, E. Obayashi, H. Yoshida, K. Sugiyama, S.Y. Park, J. Sekine, T. Urano, G196 epitope tag system: a novel monoclonal antibody, G196, recognizes the small, soluble peptide DLVPR with high affinity, Sci. Rep. 7 (2017) 43480 https://doi.org/10.1038/srep43480.

[22] H. Yoshida, S.Y. Park, T. Oda, T. Akiyoshi, M. Sato, M. Shirouzu, K. Tsuda, K. Kuwasako, S. Unzai, Y. Muto, T. Urano, E. Obayashi, A novel 3' splice site recognition by the two zinc fingers in the U2AF small subunit, Genes Dev. 29 (2015) 1649–1660 https://doi.org/10.1101/gad.267104.115.

[23] K. Konishi, F. Tanabe, M. Taniguchi, H. Yamauchi, T. Tanimoto, M. Ikeda, K. Orita, M. Kurimoto, A simple and sensitive bioassay for the detection of human inter-leukin-18/interferon-gamma-inducing factor using human myelomonocytic KG-1 cells, J. Immunol. Methods 209 (1997) 187–191 https://doi.org/10.1016/S0022-1759(97)00164-6.

[24] C. Beekman, A.A. Janson, A. Baghat, J.C. van Deutekom, N.A. Datson, Use of ca-pillary Western immunoassay (Wes) for quantification of dystrophin levels in ske-letal muscle of healthy controls and individuals with Becker and Duchenne mus-cular dystrophy, PLoS One 13 (2018) e0195850 https://doi.org/10.1371/journal.pone.0195850.

[25] I.G. Macara, Transport into and out of the nucleus, Microbiol. Mol. Biol. Rev. 65 (2001) 570–594 https://doi.org/10.1128/mmbr.65.4.570-594.2001.

[26] M. Gerfaud-Valentin, Y. Jamilloux, J. Iwaz, P. Sève, Adult-onset Still's disease, Autoimmun. Rev. 13 (2014) 708–722 https://doi.org/10.1016/j.autrev.2014.01.058.

[27] R. Giacomelli, P. Ruscitti, Y. Shoenfeld, A comprehensive review on adult onset Still's disease, J. Autoimmun. 93 (2018) 24–36 https://doi.org/10.1016/j.jaut.2018.07.018.

[28] S. Mitrovic, B. Fautrel, New Markers for Adult-Onset Still's Disease, Joint Bone Spine 85 (2018) 285–293 https://doi.org/10.1016/j.jbspin.2017.05.011.

[29] A. Feist, S. Mitrovic, B. Fautrel, Mechanisms, biomarkers and targets for adult-onset Still's disease, Nat. Rev. Rheumatol. 14 (2018) 603–618 https://doi.org/10.1038/s41584-018-0081-x.

[30] Y. Kawaguchi, H. Terajima, M. Harigai, M. Hara, N. Kamatani, Interleukin-18 as a novel diagnostic marker and indicator of disease severity in adult-onset Still's dis-ease, Arthritis Rheum. 44 (2001) 1716–1717 https://doi.org/10.1002/1529-0131(200107)44:7<1716::Aid-art298>3.0.Co;2-i.

[31] M. Kawashima, M. Yamamura, M. Taniai, H. Yamauchi, T. Tanimoto, M. Kurimoto, S. Miyawaki, T. Amano, T. Takeuchi, H. Makino, Levels of interleukin-18 and its binding inhibitors in the blood circulation of patients with adult-onset Still's dis-ease, Arthritis Rheum. 44 (2001) 550–560 https://doi.org/10.1002/1529-0131(200103)44:3<550::AID-ANR103>3.0.CO;2-5.

[32] J.H. Choi, C.H. Suh, Y.M. Lee, Y.J. Suh, S.K. Lee, S.S. Kim, D.H. Nahm, H.S. Park, Serum cytokine profiles in patients with adult onset Still's disease, J. Rheumatol. 30 (2003) 2422–2427.

[33] D.Y. Chen, J.L. Lan, F.J. Lin, T.Y. Hsieh, Proinflammatory cytokine profiles in sera and pathological tissues of patients with active untreated adult onset Still's disease, J. Rheumatol. 31 (2004) 2189–2198.

[34] T. Sugiura, N. Maeno, Y. Kawaguchi, S. Takei, H. Imanaka, Y. Kawano, H. Terajima-Ichida, M. Hara, N. Kamatani, A promoter haplotype of the interleukin-18 gene is associated with juvenile idiopathic arthritis in the Japanese population, Arthritis Res. Ther. 8 (2006) R60 https://doi.org/10.1186/ar1930.

[35] P. Conigliaro, R. Priori, M. Bombardieri, C. Alessandri, F. Barone, C. Pitzalis, I.B. McInnes, G. Valesini, Lymph node IL-18 expression in adult-onset Still's disease, Ann. Rheum. Dis. 68 (2009) 442–443 https://doi.org/10.1136/ard.2008.093781.

[36] J. Maruyama, S. Inokuma, Cytokine profiles of macrophage activation syndrome

[37] S. Colafrancesco, R. Priori, C. Alessandri, C. Perricone, M. Pendolino, G. Picarelli, G. Valesini, IL-18 Serum Level in Adult Onset Still's Disease: A Marker of Disease Activity, Int. J. Inflamm. 2012 (2012) 156890 https://doi.org/10.1155/2012/156890.

[38] K.H. Jung, J.J. Kim, J.S. Lee, W. Park, T.H. Kim, J.B. Jun, D.H. Yoo, Interleukin-18 as an efficient marker for remission and follow-up in patients with inactive adult-onset Still's disease, Scand. J. Rheumatol. 43 (2014) 162–169 https://doi.org/10.3109/03009742.2013.824023.

[39] C. Girard, J. Rech, M. Brown, D. Allali, P. Roux-Lombard, F. Spertini, E.J. Schiffrin, G. Schett, B. Manger, S. Bas, G. Del Val, C. Gabay, Elevated serum levels of free interleukin-18 in adult-onset Still's disease, Rheumatology 55 (2016) 2237–2247 https://doi.org/10.1093/rheumatology/kew300.

[40] P.H. Hirel, M.J. Schmitter, P. Dessen, G. Fayat, S. Blanquet, Extent of N-terminal methionine excision from Escherichia coli proteins is governed by the side-chain length of the penultimate amino acid, Proc. Natl. Acad. Sci. U.S.A. 86 (1989) 8247–8251 https://doi.org/10.1073/pnas.86.21.8247.

[41] H. Dalbøge, S. Bayne, J. Pedersen, In vivo processing of N-terminal methionine in E. coli, FEBS Lett. 266 (1990) 1–3 https://doi.org/10.1016/0014-5793(90)90001-B.

[42] A. Kwak, Y. Lee, H. Kim, S. Kim, Intracellular interleukin (IL)-1 family cytokine processing enzyme, Arch Pharm. Res. (Seoul) 39 (2016) 1556–1564 https://doi.org/10.1007/s12272-016-0855-0.

[43] J.A. Gracie, S.E. Robertson, I.B. McInnes, Interleukin-18, J. Leukoc. Biol. 73 (2003) 213–224 https://doi.org/10.1189/jlb.0602313.

[44] S. Sugawara, A. Uehara, T. Nochi, T. Yamaguchi, H. Ueda, A. Sugiyama, K. Hanzawa, K. Kumagai, H. Okamura, H. Takada, Neutrophil proteinase 3-medi-ated induction of bioactive IL-18 secretion by human oral epithelial cells, J. Immunol. 167 (2001) 6568–6575 https://doi.org/10.4049/jimmunol.167.11.6568.

[45] N.V. Rao, N.G. Wehner, B.C. Marshall, W.R. Gray, B.H. Gray, J.R. Hoidal, Characterization of proteinase-3 (PR-3), a neutrophil serine proteinase. Structural and functional properties, J. Biol. Chem. 266 (1991) 9540–9548.

[46] S. Kikkawa, M. Matsumoto, K. Shida, Y. Fukumori, K. Toyoshima, T. Seya, Human macrophages produce dimeric forms of IL-18 which can be detected with mono-clonal antibodies specific for inactive IL-18, Biochem. Biophys. Res. Commun. 281 (2001) 461–467 https://doi.org/10.1006/bbrc.2001.4378.

[47] Y. Yamamoto, Z. Kato, E. Matsukuma, A. Li, K. Omoya, K. Hashimoto, H. Ohnishi, N. Kondo, Generation of highly stable IL-18 based on a ligand-receptor complex structure, Biochem. Biophys. Res. Commun. 317 (2004) 181–186 https://doi.org/10.1016/j.bbrc.2004.03.024.

[48] B. Krumm, X. Meng, Y. Li, Y. Xiang, J. Deng, Structural basis for antagonism of human interleukin 18 by poxvirus interleukin 18-binding protein, Proc. Natl. Acad. Sci. U.S.A. 105 (2008) 20711–20715 https://doi.org/10.1073/pnas.0809086106.

[49] B. Krumm, X. Meng, Z. Wang, Y. Xiang, J. Deng, A unique bivalent binding and inhibition mechanism by the yatapoxvirus interleukin 18 binding protein, PLoS Pathog. 8 (2012) e1002876 https://doi.org/10.1371/journal.ppat.1002876.